ACS APPLIED MATERIALS & INTERFACES

Research Article

www.acsami.org

Direct Intense Pulsed Light Sintering of Inkjet-Printed Copper Oxide Layers within Six Milliseconds

Hyunkyoo Kang,*[,†] Enrico Sowade,[†] and Reinhard R. Baumann*[,†,‡]

[†]Digital Printing and Imaging Technology, Institute for Printing and Media Technology, Technische Universität Chemnitz, Reichenhainer Strasse 70, 09126 Chemnitz, Germany

[‡]Department Printed Functionalities, Fraunhofer Research Institute for Electronic Nano Systems (ENAS), Technologie-Campus 3, 09126 Chemnitz, Germany

Supporting Information

ABSTRACT: We demonstrate intense pulsed light (IPL) sintering of inkjet-printed CuO layers on a primer-coated porous PET substrate to convert the electrically insulating CuO into conductive Cu. With this approach, conductive layers are obtained in less than 1 s after the printing process. The IPL sintering was performed for high productivity with minimum duration and repetition of IPL irradiation to evaluate the effect of pulse number and energy output on the conductivity and morphology of the sintered Cu layers. Depending on the energy output, sheet resistances were measured as 0.355, 0.131, and 0.121 $\Omega\cdot\square^{-1}$ by exposure energy of 5.48 (single pulse), 7.03 (double pulse), and 7.48 $J\cdot cm^{-2}$ (triple pulse), respectively. In contrast, an excessive energy with relatively short pulse duration causes a delamination of the Cu layer. The lowest resistivity of about 55.4 n$\Omega\cdot$m (corresponds to about 30% conductivity of bulk Cu) was obtained by an IPL sintering process of 0.26 s after the printing, which was composed of 2 ms triple pulses with 10 Hz frequency.

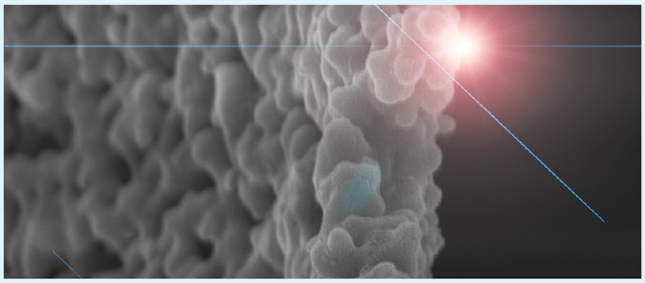

KEYWORDS: *intense pulsed light sintering, inkjet printing, copper oxide, roll-to-roll printing, printed electronics*

INTRODUCTION

Recently, inkjet printing processes, which employ either metal nanoparticles (NPs) or organic materials for functional patterning have been attracting much interest for different applications in the field of printed electronics, such as RFID tags, capacitors, rectifiers, organic thin film transistors (OTFTs), and many others.[1−5] In contrast to the traditional production of electronics such as lithography or vapor deposition, inkjet printing technology enables the fabrication of electronic circuitry with low cost, high throughput, and large-area processing on flexible materials.[6] It is an additive process and thus considered as more environmental friendly and material-saving than conventional photolithographic methods.[7] Additionally, inkjet printing technology facilitates the adaptation of roll-to-roll (R2R) production for mass manufacturing.

For solution-based manufacturing technologies such as inkjet printing, post-treatment processes play an important role. After deposition of the materials, drying, curing, or sintering steps are required to obtain a functional layer or functional devices. In many cases, even a combination of these post-treatment steps is necessary and the deposited materials as well as the substrate are exposed to high energy (usually thermal energy), for example, to enable a sinter process of metal NP. By using metal NP inks, the energy required to sinter the metal NP is dramatically reduced in comparison to the bulk metal. The conventional approach for sintering is a simple heating process on a hot plate or in oven. Usually, temperatures between 150 and 300 °C are required for high conductivity.[8] However, these temperatures are still higher than the glass transition temperature (GT) of most of the cost-effective polymer foils which are traditionally applied in graphic industry, and are also of high relevance for printed electronics, for example, polyethylene terephthalate (PET), polyethylene (PE), or polypropylene (PP). Thus, alternative technologies for the post-treatment of deposited layers were introduced to reduce the temperature affecting the stability of the polymer substrates. Possible technologies are microwave, plasma, and intense pulsed light (IPL) sintering (also called photonic sintering), or even its combinations. These technologies allow the application of cost-effective polymer foils (no destructive heating) as substrates and additionally the shortening of processing duration. Table 1 summarizes the required durations of different post-treatment methods for deposited Ag NP inks with corresponding conductivity of the layers comparing to bulk silver.[9−13]

As shown exemplary in the table, the combination of IPL and microwave exposure facilitates the shortest sintering time of 15 s for Ag NPs and a comparable high conductivity.[9] In case of R2R printing, the 15 s duration results in a considerably low

Received: October 17, 2013
Accepted: January 16, 2014
Published: January 16, 2014

Table 1. Posttreatment Technologies for Ag Nanoparticles Inks, Its Durations and the Obtained Conductivity As Ratio of Ag Bulk Conductivity

	intense pulsed light and microwave sintering[9]	microwave sintering[10]	intense pulsed light sintering[11]	plasma and microwave sintering[12]	conventional oven sintering[13]
duration (S)	15	60	300	300	1800
bulk Ag conductivity ratio (%)	40	34	34	60	30

velocity of a moving substrate in a fixed length of post-treatment process. For instance, a post-treatment length of 3 m would correspond to a comparable low operating velocity of 0.2 m/s. This low processing velocity reduces dramatically the productivity and influences finally also the production costs. Therefore, mainly high-cost substrates, such as polyimide (PI) or metal foils, were employed for electronic applications when using R2R printing processes. To enable the fabrication of R2R-printed electronics based on cost-effective polymer substrates, the existing post-treatment processes have to be well adjusted.

IPL sintering has been introduced a couple of years ago as a promising tool for printed electronics. This technology was formerly developed for the silicon industry and could recently extend its application toward printed electronics for the sintering of Ag NPs, copper oxide (CuO) NPs, and composite materials in ambient conditions.[14] Especially for printed electronics, IPL sintering technology has many benefits in comparison to traditional curing processes. Most of the traditional sintering processes such as simple thermal heating on a hot plate or in an oven applying heat to entire materials including the substrate. In contrast, IPL sintering is a more selective sintering method as it heats mainly the deposited materials by exposure of broadband light in microsecond scale.[8] Therefore, it is possible to prevent thermal defects on the substrate and reduce the very long and sophisticated paths of post-treatment processes usually employed in traditional heating concepts for R2R printing systems. In literature, the focus of IPL sintering investigations is mainly set on the effect of exposure energy or pulse shape on the conductivity of sintered layer.[15,16] But also the properties of the substrate as well as the printing and drying process play a key role for IPL sintering. In sharp contrast with the conventional curing that is usually drying and sintering the deposited wet layer for a comparable long period of time, IPL exposure aims for drying and sintering within micro- or milliseconds. The condition of the deposited layer is important for the IPL process. In literature, most of the printed layers were dried before exposing them to IPL.[14−16] In these cases, the post-treatment process is separated in a drying part and a sintering part. Using wet layers for IPL sintering is also possible and especially beneficial for R2R printing, but the process conditions need to be tuned carefully and usually higher energies and longer durations are required to vaporize the solvents and sinter the NP afterward.[17,18] That is the reason why either IPL or a combination of IPL and microwave treatment only shorten the sintering duration to 15 s in which both drying and sintering are taking place.[9]

RESULTS AND DISCUSSION

In this paper, IPL sintering of inkjet-printed CuO layers on a primer-coated porous PET substrate is demonstrated. The duration for the conductive layer formation is less than 1 s and comprises both layer drying and layer sintering. In contrast to the most research works in literature, we do not use a special drying process to vaporize solvents of the deposited inks before the IPL process, because the porous substrate can partially absorb the deposited solvent, which results to optimized conditions for the sintering process. Next to the solvent absorption, the porous substrate has a second important function: It supports the leveling of the printed layers to a certain extend leading to smoother layer morphologies in contrast to nonporous substrates. Furthermore, also the adhesion of the layer is improved which is important for IPL sintering. The conductivity as well as the morphology of sintered copper (Cu) layers were analyzed according to the IPL parameters such as energy exposure, pulse length, and number of pulses.

IPL sintering for high productivity with minimum duration and repetition of IPL irradiation was performed to evaluate the effect of pulse number and energy on the conductivity and morphology of the sintered Cu layer on the porous substrate. As it was mentioned above, the productivity of a R2R system mainly depends on the time duration of the post-treatment process for the deposited layers. In case of IPL sintering, the productivity of the R2R system is determined by the number of pulses and the frequency. The number of pulses was set to 1, 2, and 3 with a constant total duration of 6 ms and a fixed frequency of 10 Hz (see Supporting Information Figure S3a−c for further details). For high productivity, IPL sintering should have as less pulses as possible and a high frequency. Figure 1 shows the obtained sheet resistances of IPL sintered Cu as a function of energy exposure. The sheet resistance of Cu is reversely proportional to the energy exposure of the IPL. When the exposed energy is less than 3.98 J·cm^{-2}, sintering of the

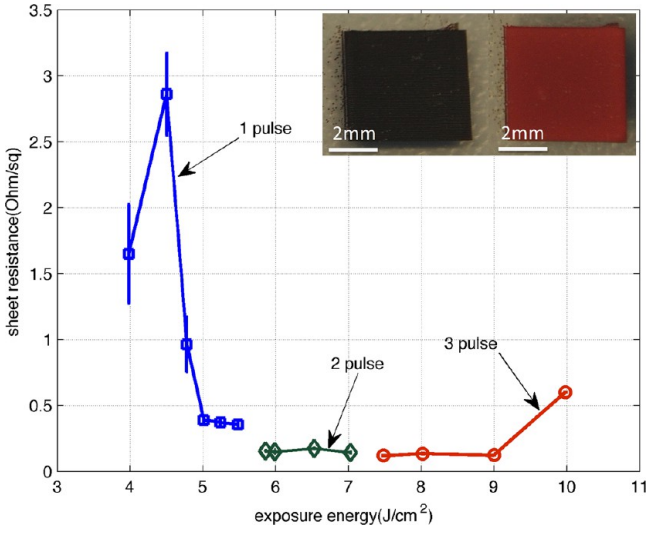

Figure 1. Sheet resistance of sintered Cu layer as function of energy exposure and number of pulses. The frequency for multi pulses is 10 Hz and the pulse duration 6 ms. The inset shows a macrophotograph of square patterns of as-printed CuO (left, not conductive) and IPL-sintered Cu (right, conductive).

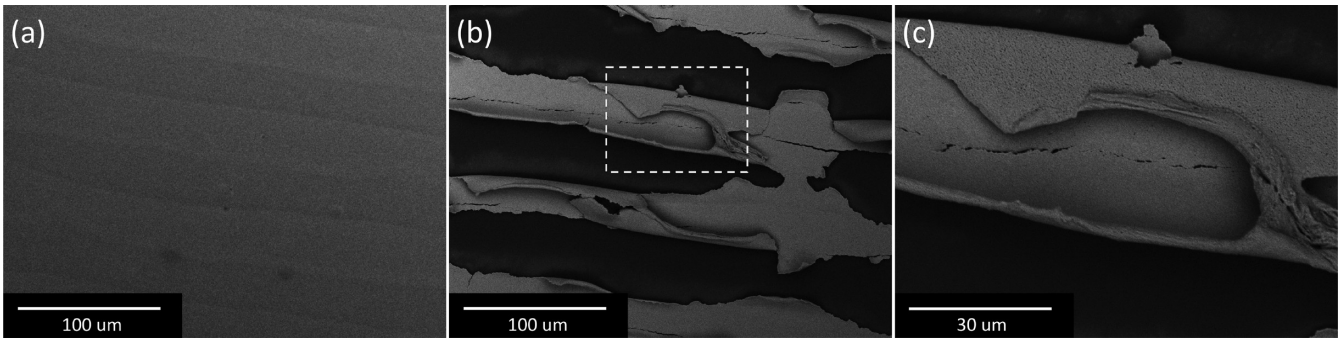

Figure 2. (a) Scanning electron microscopy (SEM) images of IPL-sintered Cu layers of a well-sintered pattern, (b) a delaminated Cu layer in which the delamination follows the printing paths, and (c) a magnification of the marked area of b to show the roll-up of the printed layer after IPL sintering with high energy.

CuO layer is not possible. The energy is too low for solvent vaporization, the chemical reduction of CuO as well as elimination of its organic stabilizers and the sintering process. Using a single pulse of 3.98−5.48 J·cm^{-2}, the sheet resistance was measured as 0.355−2.861 Ω·□$^{-1}$. Energies higher than 5 J·cm^{-2} within one single pulse decrease dramatically the sheet resistance. The sheet resistance was measured to 0.131−0.172 Ω·□$^{-1}$ for a double pulse in the range of 5.86−7.03 J·cm^{-2}. For a triple pulse of 7.48−9.98 J·cm^{-2}, the sheet resistance was measured as 0.121−0.599 Ω·□$^{-1}$.

It is noteworthy, that excessive energy with relatively short pulse duration causes a delamination of the Cu layer, for example, for more than 5.86 J·cm^{-2} in a single pulse (duration is 6 ms) or more than 7.48 J·cm^{-2} for a double pulse (duration of each pulse is 3 ms). In these cases, the Cu layer is partially delaminated from the substrate as shown in Figure 2b and 2c, the sheet resistance of which was measured as 4.57 MΩ·□$^{-1}$. The delamination follows the droplet path by printing direction, thus depends strongly on the conditions of droplet deposition. Normally, the deposited droplets coalescence and accumulate as a wet film when using nonporous substrates. We call this "wet-in-wet printing". The topography of the deposited layer, after drying, is determined by the conditions of evaporation (e.g., vaporization on the surface and fluidic circulation).[21] In contrast, a droplet on porous substrate is pinned immediately after the contact with the substrate due to the solvent absorption, which initiates the drying of the droplet. When ejecting the next droplet in printing direction, the drop will coalesce with the former one because pinning and drying has not been advancing much. Droplets printed in the same line in printing direction will thus coalescence. When printing of the first line finishes, the print head will go back to starting position and will begin with the second line. Because of the movement of the print head, a certain time of period will pass. During this period, the former printed line is pinned and drying advanced. The droplets deposited in the second line will thus not coalesce with the droplets printed before but leading to clearly visible lines in the printed pattern as shown in Supporting Information Figure S1b and c. Figure 2b shows the delamination of the Cu layer. Obviously, the delamination follows the droplet path caused by the deposition process. The rapid evaporation of solvents and binders of the CuO ink during the IPL exposure can initiate the delamination.[16] Furthermore, the inhomogeneous layer of the deposited CuO showing clearly lines from the inkjet printing process contributes to an irregular absorption of energy. In case of higher layer thickness, the energy absorption might be intensified resulting in delamination at these areas. Former research on IPL sintering of Cu and Ag demonstrated, that the delamination of sintered layers can be prevented by multistep sintering with 8−16 pulses.[15,22] However, this strategy is not qualified to enable the application of IPL sintering for high productivity, for example, R2R manufacturing. If the required number of pulses increases, the operating velocity of the system has to be decreased in constant frequency of IPL, which is physically limited due to capacitor charging period in continuous irradiations. Therefore, we suggest less number of pulses for high productivity as well as prevention of delamination by fine-tuning of IPL process parameters.

Figure 3a−3d show the SEM images of as-printed CuO and sintered Cu layers at different IPL exposure energies. The SEM images b−d clearly demonstrate that the Cu NPs are agglomerated and a continuous conductive network is formed. The increasing irradiation energy applied results to grain size growth and to smaller pores, which finally improves the conductivity as already shown in Figure 1. Figure 3b shows more pores than Figure 3c because grains of Cu grew and neck formation is initiated with increasing IPL exposure energy. The pores in Figure 3b can interrupt the electron transfer and decrease the conductivity. In Figure 3c, the area as well as the number of pores were reduced and branches of Cu NPs were formed because of the higher energy irradiation of 5.99 J·cm^{-2}. Figure 3d shows a complex network of Cu with increased grains. The number of pores increased, but the pore sized decreased contributing to higher conductivity. The bonding of the particles to each other and the grain growth finished. It is not possible to decrease the remaining porosity using IPL. Higher energies cause delamination and thus the layer is destroyed and conductivity increases. A detailed study about the grain growth and neck formation of the Cu particles based on image processing can be found in Supporting Information Figure S4. Figure 3e shows the energy dispersive X-ray (EDX) analysis of an as-printed CuO and IPL-sintered Cu layer according to the different energy exposures. It clearly shows, that the oxygen (O) of the inkjet-printed CuO layer and organic stabilizers were reduced by the IPL exposure, even with the lowest energy of 5 J·cm^2. According to the graph, the different energies of IPL exposure have no influence on the amount of oxygen reduction. The mechanism of the reduction of CuO to pure Cu using IPL sintering is barely studied in literature and thus not yet sufficiently clarified. Ryu at el.[23] propose a reactive sintering mechanism because of photoactive polymers that act like alcohol or acid reductants during the IPL process and enable the reduction of the CuO shell to Cu.

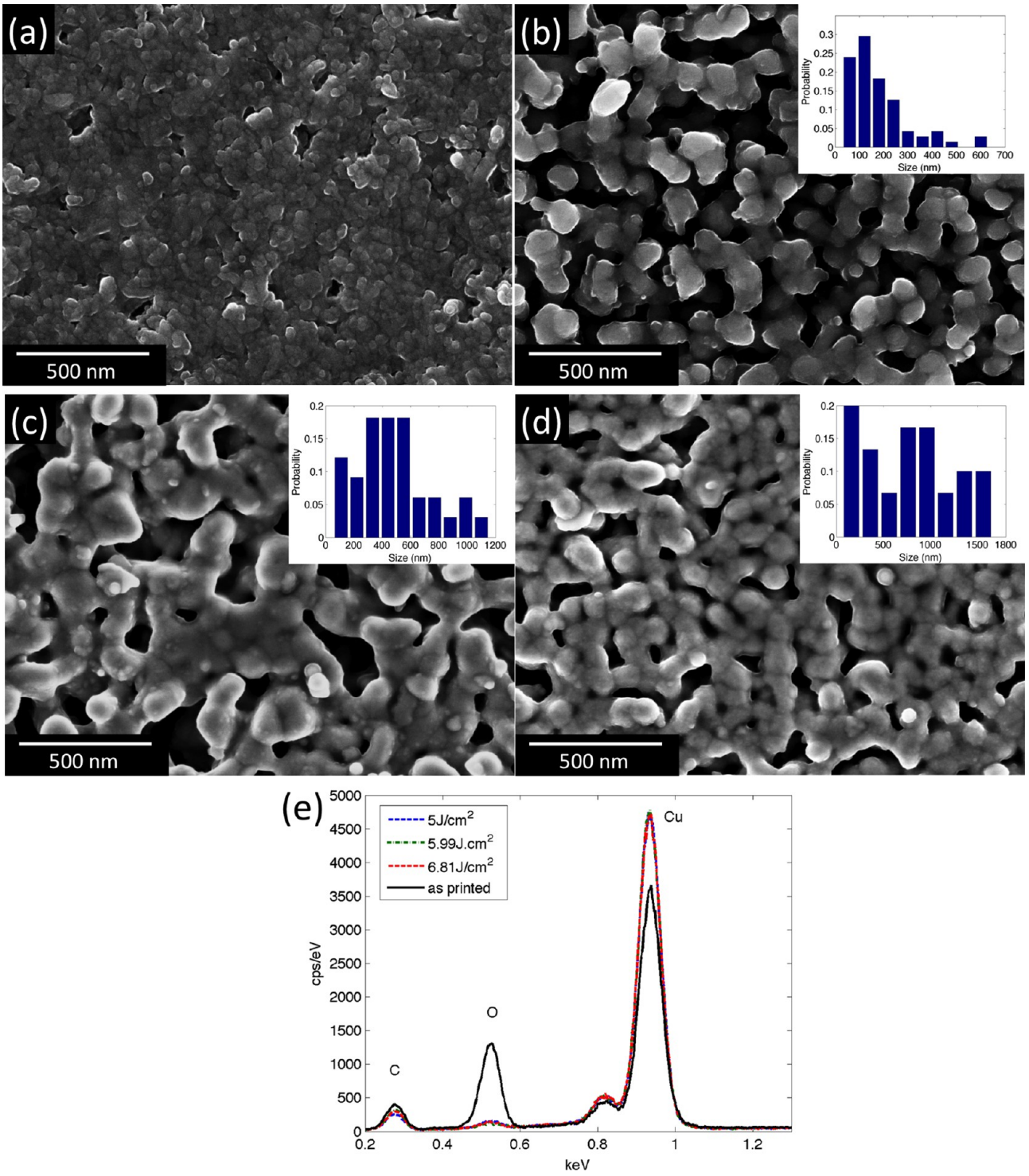

Figure 3. Scanning electron microscopy (SEM) images of (a) as-printed CuO layer and IPL-sintered Cu layers of different exposure energies: (b) 5.01 J·cm^{-2} by 1 pulse, (c) 5.99 J·cm^{-2} by 2 pulses, and (d) 6.81J.cm^{-2} by 3 pulses. The insets show graphs of pores probability as function of pore size obtained by the linear intercept method. (e) Energy dispersive X-ray (EDX) analysis of as-printed CuO and sintered Cu layers of panels a–d.

However, further studies on the CuO reduction using IPL are required to have a verified and exact explanation of mechanism.[23]

Higher energy of IPL forms much more dense structures of Cu NPs, which results to higher conductivity. However, the number and duration of pulses has to be controlled to prevent the delamination.

The layer thickness of the sintered Cu layers as a function of the IPL energy is illustrated in Figure 4a. The thickness of the inkjet-printed CuO layer without any treatments was measured to about 1020 ± 70 nm. The thickness of the sintered Cu layer decreases as the exposure energy increases. With a single pulse of 3.98–5.48 J·cm^{-2}, the thickness was reduced to about 1020–500 nm. In case of double pulses of 5.86–7.03 J·cm^{-2}, the thickness was decreased to 650–450 nm. However, for the

dx.doi.org/10.1021/am404581b | ACS Appl. Mater. Interfaces 2014, 6, 1682–1687

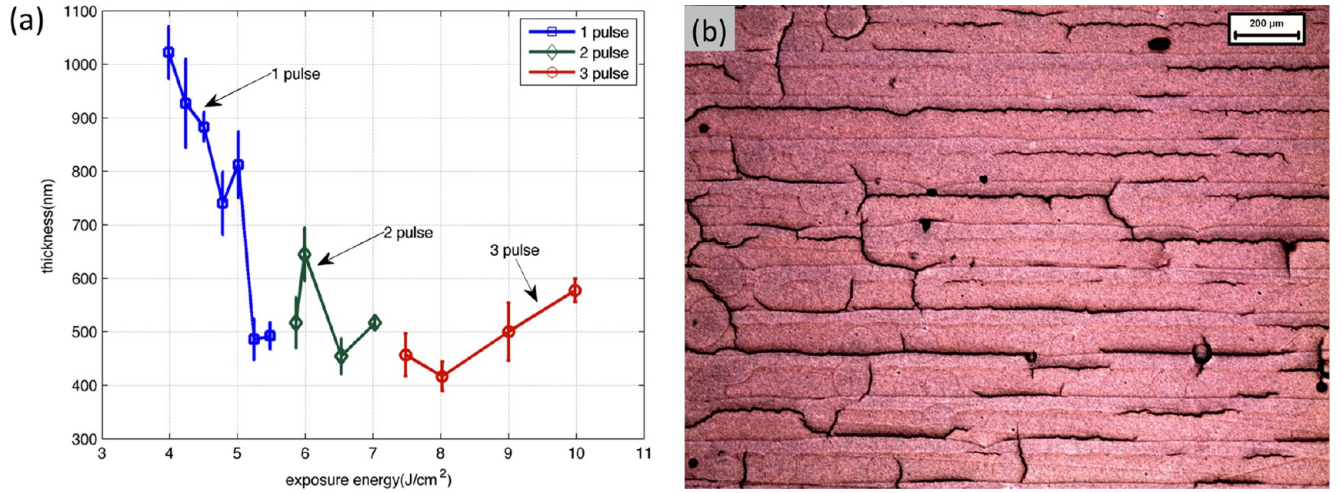

Figure 4. (a) Thickness of IPL-sintered Cu layer as function of energy exposure and (b) microscope image of cracks along droplet path with curled edge in IPL-sintered Cu layer at 9.98 J·cm^{-2}.

higher energies used in the triple pulse, the thickness increased again up to 580 nm. This is because of the formation of huge grains in the Cu layer, which induced inhomogeneous shear force along the droplet printing path for delamination from the substrate. In the microscopic image of Figure 4b, it can be verified that cracks along the droplet path as well as curled edges occurred when using excessive irradiation energy.

The lowest resistivity of IPL sintered Cu layers can be calculated to about 55.4 nΩ·m, which is about 30% of bulk Cu conductivity. The sheet resistance is 0.132 Ω·□$^{-1}$ and the layer thickness 420 nm. The layer was IPL-sintered at 8 J·cm^{-2}. To verify the applicability of the proposed IPL sintering method, a RFID coil pattern was inkjet-printed and sintered as demonstrated in Figure 5 (using a single pulse of 4.5 J·cm^{-2}).

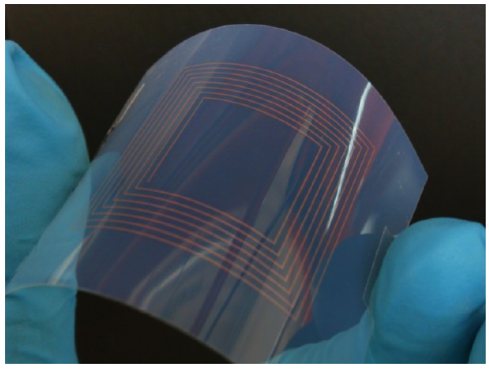

Figure 5. Inkjet-printed Cu coil pattern on porous PET substrate.

CONCLUSIONS

In conclusion, we reported about IPL sintering of inkjet-printed CuO layers on a primer-coated porous PET substrate. Because of the IPL sintering, the CuO was converted into Cu with up to 30% conductivity of bulk Cu within 6 ms. In contrast to most research works in literature, we do not use a special drying process to vaporize solvents of the deposited inks before the IPL process. The porous substrate used here can partially absorb the deposited solvent which results in optimized conditions for the sintering process. Furthermore, also the adhesion of the Cu is improved using the primer-coated substrate, which is important for IPL sintering. The conductivity, as well as the morphology, of sintered Cu layers were analyzed according to IPL parameters such as energy exposure, pulse length, and number of pulses. The duration for the conductive layer formation is less than 1 s and comprises both layer drying and layer sintering. In addition, the layer formation is also possible on flexible and cheap polymer substrates as demonstrated. Both the very short sintering duration and the flexible polymer substrates can be considered as important step toward R2R processing and higher productivity.

MATERIALS AND METHODS

For the investigation of Cu layers on the porous PET substrate, a commercially available water-based CuO ink (ICI-002HV, NovaCentrix) with 16 wt % solids content was used. The CuO ink was percolated by a polytetrafluoroethylene (PTFE) filter with a pore size of 1 µm before deposition by an inkjet printer. One side primer-coated PET foil (IJ-220, NovaCentrix) was employed as porous substrate. The primer is a sol–gel applied silica layer which is commonly used as absorptive coating for inkjet substrates in graphic industries. It is a hydrophilic material with fine porosity providing high absorption capacity for fluids. In graphic inkjet industry, the silica-coated substrates are mainly used for high quality color printing contributing to optimized optical density and color gamut.

The SEM image of the primer-coated substrate reveals a notable nanostructure with many pores for the absorption of deposited ink as shown in Supporting Information Figure S1a. For the SEM image, the primer-coated PET was sputtered with about 15 nm Pt. The structure of Pt intensifies the structure of the primer coating. The grain and gap sizes of the coating were measured by the linear intercept method to about 75 ± 4 and 22 ± 4 nm, respectively.[19] For the linear intercept method, five horizontal lines were depicted in the SEM image, where the boundaries between grain and gap were determined. Then, by comparing relationship between scale bar and pixel number, the grain and gap were calculated using numerical calculation software, MATLAB (MathWorks). The Autodrop deposition system manufactured by Microdrop Technology was employed to print the prepared CuO ink in squares of 5 × 5 mm^2 as shown in Supporting Information Figure S2a. The system was equipped with a piezoelectric inkjet single nozzle (MD-K-130) having a nozzle orifice diameter of 69 µm. Printing parameters of drop spacing, printing velocity and printing direction were adjusted as 80 µm, 25 mm·s^{-1}, and one way printing (printing origin is every time on the same side, the pattern is developed line by line), respectively. In case of the printed coil of Figure 5, the printing direction was not line by line, but was following

dx.doi.org/10.1021/am404581b | ACS Appl. Mater. Interfaces 2014, 6, 1682–1687

the drawing path of the coil (from the outside to the center). The inkjet-printed CuO layers were sintered by the IPL sintering system PulseForge 3200 (NovaCentrix, Supporting Information Figure S2b), at room temperature and in ambient condition. The IPL sintering system is designed for R2R processing and consists of four xenon lamps, a reflector system and a water-cooled metal back-plate.[20] The exposure energy of a single pulse can be adjusted from 0.01 to 15 J·cm^{-2} by variation of two parameters: Voltage and pulse duration. The voltage and the pulse duration were adjusted between 150 and 390 V and 30 μs and 10 ms, respectively. Also multipulses with a frequency range of 0.01 Hz−50 kHz are possible.

The layer surface and cross sections were characterized by optical microscopy using a Leica DM4000 M microscope and by SEM using a FEI Nova NanoSEM 200. For the measurement of sheet resistance, a 4-point probe station (PM5, Süss Microtec) with source meter (2636A, KEITHLEY) was employed. The layer morphology of the sintered Cu was measured using a surface profilometer (Dektak 150, Veeco).

■ ASSOCIATED CONTENT

Supporting Information

SEM image of primer-coated porous substrate, microscopic images of as-deposited CuO layers, macroscopic images of inkjet printing system and IPL sintering module, the pulse profiles for the IPL process, and measurements of percentage of pores in the IPL sintered Cu layer. This information is available free of charge via the Internet at http://pubs.acs.org/.

■ AUTHOR INFORMATION

Corresponding Authors

*E-mail: hyunkyoo.kang@mb.tu-chemnitz.de
*E-mail: reinhard.baumann@mb.tu-chemnitz.de.

Notes

The authors declare no competing financial interest.

■ ACKNOWLEDGMENTS

This work was financially supported by the Alexander von Humboldt Foundation. The authors kindly acknowledge Torsten Jagemann (Chair of Solid Surfaces Analysis at TU Chemnitz under Prof. Hietschold) and Cornelia Kowol (Department of Layer Deposition at Fraunhofer ENAS) for their support with SEM and EDX analysis and the sample preparation.

■ REFERENCES

(1) Jalkanen, T.; Makila, E.; Maattanen, A.; Tuura, J.; Kaasalainen, M.; Lehto, V.; Ihalainen, P.; Peltonen, J.; Salonen. *J. Appl. Phys. Lett.* **2012**, *101*, No. 263110.
(2) Pranonsatit, S.; Worasawate, D.; Sritanavut, P. *IEEE Trans. Compon. Packag. Technol.* **2012**, *2*, 878−883.
(3) Allen, M.; Lee, C.; Ahn, B.; Kololuoma, T.; Shin, K.; Ko, S. *Microelectron. Eng.* **2011**, *88*, 3293−3299.
(4) Skotadis, E.; Tang, J.; Tsouti, V.; Tsoukalas, D. *Microelectron. Eng.* **2010**, *87*, 2258−2263.
(5) Marjanovic, N.; Hammerschmidt, J.; Perelaer, J.; Farnsworth, S.; Rawson, I.; Kus, M.; Yenel, E.; Tilki, S.; Schubert, U. S.; Baumann, R. R. *J. Mater. Chem.* **2011**, *21*, 13634−13639.
(6) Sheats, J. R. *J. Mater. Res.* **2004**, *19*, 1974−1989.
(7) Xu, J. M. *Synth. Met.* **2000**, *115*, 1−3.
(8) Kamyshny, A.; Steinke, J.; Magdassi, S. *Open Appl. Phys. J.* **2011**, *4*, 19−36.
(9) Perelaer, J.; Abbel, R.; Wünscher, S.; Jani, R.; Lammeren, T. V.; Schubert, U. S. *Adv. Mater.* **2012**, *24*, 2620−2625.
(10) Perelaer, J.; Klokkenburg, M.; Hendriks, C. E.; Schubert, U. S. *Adv. Mater.* **2009**, *21*, 4830−4834.
(11) Kang, J. S.; Ryu, J.; Kim, H. S.; Hahn, H. T. *J. Electron. Mater.* **2011**, *40*, 2268−2277.
(12) Perelaer, J.; Jani, R.; Grouchko, M.; Kamyshny, A.; Magdassi, S.; Schubert, U. S. *Adv. Mater.* **2012**, *24*, 3993−3998.
(13) Kim, D.; Moon, J. *Electrochem. Solid State* **2005**, *8*, J30−J33.
(14) Kim, H. S.; Dhage, S. R.; Shim, D. E.; Hahn, H. T. *Appl. Phys. A: Mater. Sci. Process.* **2009**, *97*, 791−798.
(15) Han, W. S.; Hong, J. M.; Kim, H. S.; Song, Y. W. *Nanotechnology* **2011**, *22*, 395705.
(16) Chung, W. H.; Hwang, H. J.; Lee, S. H.; Kim, H. S. *Nanotechnology* **2013**, *24*, 035202.
(17) Reinhold, I.; Müller, M.; Müller, M.; Voit, W.; Zapka, W. *Int. Conf. Digital Print. Technol. Digital Fabr.* **2011**, 424−430.
(18) Galagana, Y.; Coenen, E. W. C.; Abbel, R.; Lammeren, T. J.; Sabik, S.; Barink, M.; Meinders, E. R.; Andriessen, R.; Blom, P. W. M. *Org. Electron.* **2013**, *14*, 38−46.
(19) Launeau, P.; Archanjo, C. J.; Picard, D.; Arbaret, L.; Robin, P. Y. *Tectonophysics* **2010**, *492*, 230−239.
(20) Schroder, K. A. *Nanotechnology* **2011**, *2*, 220−223.
(21) Deegan, R. D.; Bakajin, O.; Dupont, T. F.; Huber, G.; Nagel, S. R.; Witten, T. A. *Nature* **1997**, *389*, 827−829.
(22) Park, S. H.; Jang, S.; Lee, D. J.; Oh, J.; Kim, H. S. *J. Micromech. Microeng.* **2013**, *23*, No. 015013.
(23) Ryu, J.; Kim, H.-S.; Hahn, H. T. *J. Electron. Mater.* **2011**, *40*, 42−50.